Computer simulation of the nucleation and thermodynamics of microclusters

M. Rao and B. J. Berne[a)]

Department of Chemistry, Columbia, University, New York, New York 10027

M. H. Kalos[b)]

Courant Institute of Mathematical Sciences, New York University, New York, New York 10012
(Received 26 September 1977)

Gas liquid equilibrium in finite systems is studied by computer simulation using molecular dynamics and Monte Carlo techniques. In overexpanded liquids, cavitation is observed. At some point in the expansion the system undergoes a transition from a liquid with cavities to a droplet in equilibrium with vapor. This transition is observed in the pV diagram of the system. A method is devised for counting the number of atoms in a cluster and thereby determining the cluster distribution function. The interface of a microcluster is compared to that of a planar sheet. The two are found to be very similar in density profile. In the course of this study homogeneous nucleation in a supersaturated gas is observed for the first time in a molecular dynamics study. Simple theories of nucleation in a finite system are considered. The free energy of formation of a droplet is found to have a maximum—a barrier to nucleation—and a minimum—stable equilibrium between a droplet and liquid. When gas imperfection is included, the barrier increases, and the stable cluster is destabilized.

I. INTRODUCTION

Since the advent of high speed computers our knowledge of the liquid state has been greatly advanced using molecular dynamics and Monte Carlo techniques. Besides giving experimental data on well-defined models, these techniques are useful in obtaining information on various theoretical quantities that cannot easily be measured in the laboratory (if at all!). Currently attention is being focused on employing these techniques to study more complex problems related to interfaces, phase segregation, nucleation, etc. It is well known that a liquid coexists with its vapor in equilibrium below its critical temperature T_c. To simulate this well-defined phase separation using Monte Carlo or molecular dynamics, special boundary conditions are employed that allow one to study the asymmetry of the physical surface. Using special schemes several investigators[1-7] have succeeded in simulating the two phase systems, and these experiments have already shed a considerable amount of light on the transition zone between the two phases.

When the geometry of the interface is planar the liquid and vapor coexist in equilibrium at a pressure $P_\infty(T)$ $(T < T_c)$ called the vapor pressure. Such an interface can support capillary waves of long wavelength created by surface tension forces in the direction parallel to the surface. Recent computer experiments[7] have demonstrated the existence of these waves and provided a suitable framework for the microscopic phenomenology of two-phase fluid interfaces, together with a determination of the surface tension, σ and $P_\infty(T)$.

Homogeneous nucleation in supersaturated gases depends on an interplay between the surface and bulk properties of microclusters. Although a slightly supersaturated vapor has a higher chemical potential than bulk liquid and is thereby thermodynamically unstable, this vapor can exist indefinitely in a metastable state. When the supersaturation exceeds a certain critical value, the vapor condenses spontaneously.

For vapor to condense, clusters of microscopic size must first form. In conventional nucleation theory,[8] the free energy of formation of a spherical droplet of radius r from an infinite supersaturated gas of pressure P is found to be

$$\Delta G = 4\pi r^2\sigma - \tfrac{4}{3}\pi r^3 n_L kT \ln S \,, \tag{1}$$

where σ is the surface tension, n_L is the bulk density of the liquid droplet, $S = P/P_\infty(T) > 1$ is the supersaturation, and $P_\infty(T)$ is the equilibrium vapor pressure of bulk liquid at the temperature T. The basic assumptions that go into the derivation of Eq. (1) are (a) the vapor is an ideal gas, (b) the surface free energy $4\pi r^2\sigma$ of a microcluster can be computed using the surface tension of a macroscopic sample of liquid with a planar surface, (c) macroscopic thermodynamics can be applied to the study of microclusters, and (d) the formation of a microcluster in an infinite system does not reduce the vapor pressure.

The first term in Eq. (1) represents the work required to create a spherical surface of surface area $4\pi r^2$ and the second represents the lowering of the free energy due to the fact that the atoms in the bulk liquid have a lower free energy than in the supersaturated vapor.

It follows from Eq. (1) that as a cluster grows, ΔG first must increase because at small r the surface term dominates, then reaches a maximum $\Delta G^* = 16\pi\sigma^3/[3(n_L kT\ln S)^2]$ at the radius $r^* = (2\sigma/n_L kT\ln S)$, and for $r > r^*$ decreases without bound. In fact only in infinite systems does ΔG decrease without bound as $r \to \infty$. In finite systems a cluster does not grow without bound

a)Supported by grants to B. J. Berne from the National Science Foundation (NSF CHE 76-11002) and the National Institutes of Health (NIH-R01 NS 12714-02).
b)Supported by ERDA contract #EY-76-C-02-3077*000.

 0021-9606/78/6804-1325$01.00

and ΔG is expected to have a local minimum at some $r = r_0 > r^*$. This is shown in Sec. III, where classical nucleation theory is developed for finite systems taking into account vapor imperfection and the excluded volume of the cluster.

The foregoing suggests that there is an activation free energy barrier of high ΔG^* preventing a cluster from growing to a certain "critical cluster size," r^*. However, if the cluster grows to r^*, it has a high probability of condensing. Obviously the higher the supersaturation S, the smaller r^* and ΔG^* and the faster will liquid condense. These parameters are of fundamental importance in classical nucleation theory, where they then can be used to compute the flux of clusters over the barrier, i.e., the condensation rate. The theory has been developed only for isothermal infinite supersaturated gases.

There is much controversy surrounding this theory. One question that is often debated is whether Eq. (1) is wrong because it ignores the translational and rotational degrees of freedom of the microclusters. Another question obviously concerns the use of macroscopic thermodynamics to characterize the droplet. Even then should there not be a radius dependence in σ? We might ask yet another question: does nucleation occur in nature as an adiabatic or an isothermal process? Clearly, as particles condense the latent heat should give rise to an increase in temperature. If the supersaturated vapor is dense enough then collisions might thermostat the droplet, but is this the case? As we shall see, molecular dynamics gives evidence that gas collisions are not frequent enough to prevent the heating process in the system studied here.

Given the many questions that still exist concerning condensation—questions that are not easily answered by experiment—it would be of considerable interest to simulate these processes on a computer. To this end, we present a study of microclusters using Monte Carlo and molecular dynamics. Employing new boundary conditions we "prepare" small "physical clusters" in equilibrium with vapor and then study the structure of the gas–liquid interface, the thermodynamic properties of the system, such as how the equilibrium cluster size depends on pressure, and certain dynamic properties. In this connection we have observed the nucleation of a liquid droplet from a supersaturated gas. Our boundary conditions are different from the "constraining volume" method employed by previous[1] investigators and avoids various criticisms leveled[9,10] against their work.

This paper represents the first in a series of papers exploring condensation. In order to obtain some insight to guide us in our quest, we present, in Sec. II, a simple classical theory of nucleation in finite systems. In Sec. III, the novel boundary conditions are discussed as well as various details of the molecular dynamics and Monte Carlo techniques used. Section IV is devoted to the results.

This paper demonstrates the feasibility of simulating inhomogeneous systems consisting of droplets in equilibrium with vapor. Future studies will make use of the tools developed here with respect to boundary conditions and cluster definition. Two studies are already in progress. In the first the radial dependence of the surface tension is being studied and in the second the dynamics of droplet growth and of evaporation and condensation kinetics is probed. To understand the results in this paper an accurate thermodynamics of small systems must be developed.

II. BARRIER TO NUCLEATION IN A FINITE SYSTEM

In classical nucleation theory[3,11] one considers a uniform drop of liquid in equilibrium with an ideal gas at constant pressure $P(T)$ and temperature T. In a computer simulation the number of particles N and volume V are usually fixed so that the average density is given by N/V. In such a simulation the variation of cluster or droplet size causes a variation in the pressure of the system and this leads to a completely different picture from the classical nucleation picture. In the following we shall consider a simple model and show that in a simulation we can still identify a "critical droplet" which is appropriate to the finite system and in addition there exists a "stable droplet" whose size depends on N, V, and T. If the total free energy of the system containing a stable droplet is lower than the uniform phase, it is possible to simulate the droplet in equilibrium with its vapor and study the corresponding thermodynamics.

Let us consider a simple model in which N particles are constrained to a volume V at a temperature $T < T_c$. For large values of V if the configuration is uniform (gas phase) the pressure is given by

$$P = \bar{n} k T \left(1 + \sum_{k=1}^{\infty} B_{k+1}(T) \bar{n}^k\right), \tag{2}$$

where $\bar{n} = N/V$, and $B_{k+1}(T)$ is the $k+1$ virial coefficient. In writing Eq. (2) it is assumed that the volume is sufficiently large that the cluster integrals are volume independent. The chemical potential $\mu_G(\bar{n}, T)$ (per atom) is given by

$$\mu_G(\bar{n}, T) = \mu_G^0(T) + kT\left[\ln(\bar{n}kT) + \sum_{k=1}^{\infty}\left(\frac{k+1}{k}\right) B_{k+1}(T)\bar{n}^k\right], \tag{3}$$

and the Gibbs free energy of the gas $G_G(\bar{n}, T) = N_G \mu_G(\bar{n}, T)$. Let us consider now a simple model consisting of a spherical droplet of radius r containing N_L particles at the liquid density n_L [n_L is not the density at which an infinite sheet of liquid will be at equilibrium with its vapor at a pressure $P_\infty(T)$] in equilibrium with N_G atoms constituting the vapor phase. Clearly,

$$N_L + N_G = N. \tag{4}$$

Let the droplet be situated in the middle of the box so that we can neglect boundary effects. The N_G gas atoms are constrained to move in the volume $V - V_L(r)$ where $V_L(r) = \frac{1}{3}4\pi(r + \frac{1}{2}a)^3$ is the excluded volume due to the droplet and $a/2$ is the radius of a gas atom. Given Eq. (4) it is clear that the vapor density is

$$n_G = \frac{N - N_L(r)}{V - V_L(r)} = \left(\frac{N - \frac{1}{3}4\pi r^3 n_L}{V - V_L(r)}\right). \tag{5}$$

The total Gibbs free energy is made up of three parts:

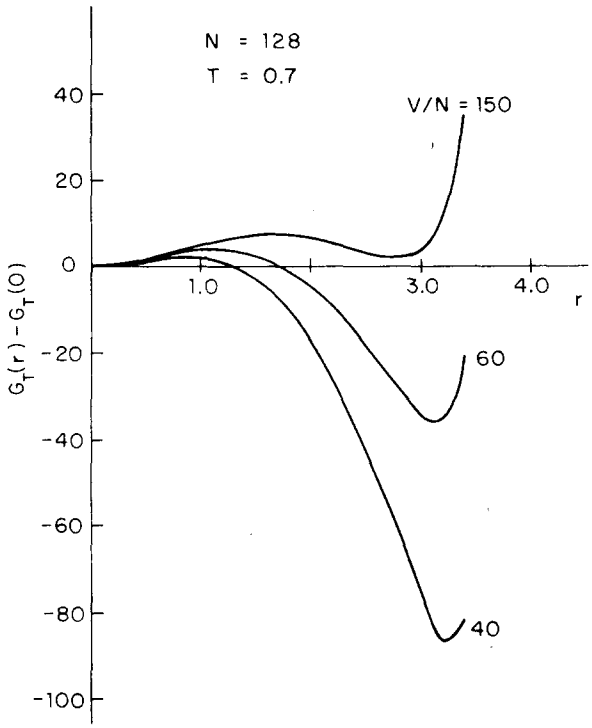

FIG. 1. Plot of excess free energy $[\Delta G_F(r)]$ as a function of r as given by Eq. (12), assuming the vapor is an ideal gas.

$$G = G\ \text{gas} + G\ \text{surface} + G\ \text{liquid}, \tag{6}$$

where

$$G\ \text{gas} = N_G \mu_G(n_G(r), T)\ , \tag{7}$$

$$G\ \text{liquid} = \mu_L(n_L, T) n_L 4\pi r^3/3\ , \tag{8}$$

$$G\ \text{surface} = 4\pi r^2 \sigma\ , \tag{9}$$

where σ is the surface tension of the droplet. Strictly speaking this should be a function of r. Note that

$$\mu_L(n_L, T) = \mu_L(n_L^\infty, T) + \frac{1}{n_L^\infty}[P(r) - P_\infty(T)]\ , \tag{10}$$

where n_L^∞ is the density of an infinite liquid sheet under its vapor pressure and $P(r)$ is the vapor pressure in a system with a droplet of radius r. Equation (10) is found by integrating $(\partial \mu_L/\partial P)_T = 1/n_L$ over pressure from $P_\infty(T)$ to P and assuming for this purpose that the liquid is incompressible. Now noting from the equilibrium condition that $\mu_L(n_L^\infty, T) = \mu_G(n_G^\infty, T)$, and substituting Eqs. (7), (8), (9), and (10) into Eq. (6) we obtain

$$G(r) = (N - N_L)\mu_G(n_G(r), T) + N_L \mu_G(n_G^\infty, T) + \frac{N_L}{n_L^\infty}[P(r) - P_\infty(T)] + 4\pi r^2 \sigma\ . \tag{11}$$

The free energy of the system in the absence of a droplet ($r = 0$, $N_L = 0$, $V_L = 0$) is $G(0) = N\mu_G(\bar{n}, T)$. The property of interest is the free energy of formation $\Delta G_F(r) = G_T(r) - G_T(0)$ of a droplet from the supersaturated gas. Substitution of Eqs. (3) into Eq. (11) then gives

$$\Delta G_F(r) = \left(N - \frac{4\pi}{3} r^3 n_L\right) kT\left[\ln\left(\frac{n_G(r)}{n_G^\infty}\right) + \sum_{k=1}^{\infty} \frac{k+1}{k} B_{k+1}(T)(n_G^k(r) - n_G^{\infty k})\right] + \frac{4\pi}{3} r^3 kT\left[n_G(r) - n_G^\infty + \sum_{k=1}^{\infty} B_{k+1}(T)[n_G(r)^k - n_G^{\infty k}]\right]\ . \tag{12}$$

If we knew all the virial coefficients we could obtain the equilibrium configuration by minimizing $\Delta G_F(r)$ subject to Eq. (5).

It is of interest to study $\Delta G_F(r)$ as a function of r for fixed N, V, T. First we assume that the vapor is an ideal gas $[B_{k+1}(T) = 0$ for all $k]$ and furthermore we use σ and n_G^∞ obtained from a molecular dynamics experiment on an infinite sheet (see Ref. 7). In Fig. 1 a plot is given of $\Delta G = (r)$ as a function of r for three values of V/N with $N = 128$ and $T = 0.7$. For the purposes of discussion we define

$$S' = \bar{n}/n_G^\infty = N/V n_G^\infty\ . \tag{13}$$

If the gas were ideal this would tell us the initial supersaturation, that is, the supersaturation in the system before a droplet forms. The three values of $V/N = 40$, 60, 150 correspond to supersaturations of $S' = 7.58$, 5.05, 2.02, respectively. For small values of V/N or equivalently for large values of S', there is a minimum in the free energy corresponding to a "stable cluster size." As V/N increases (or S' decreases), the stable cluster size decreases and the depth of the minimum decreases until at sufficiently small S', the uniform gas is more stable than a droplet and the system will not condense. In addition to the stable minimum Fig. 1 also shows that there is a maximum in the free energy. This maximum is the barrier to nucleation and its position defines the "critical cluster radius," r^*. It should be noted that as V/N increases, (S' decreases) the barrier to nucleation increases and r^* increases. This is analogous to the well-known increase of the barrier height with decreasing supersaturation in classical nucleation theory (see Sec. I). In one of the simulations reported here a gas at relatively large S' (= 9.7) was observed to nucleate rapidly. This was undoubtedly due to the very small barrier to nucleation for small V/N (high supersaturation). Were we to repeat the experiment for much larger V/N, the barrier to nucleation might be high enough to preclude nucleation on any realistic simulation time scale even though the stable state is a droplet in equilibrium with vapor. It is important to note in this connection that for finite systems the droplet radius is finite and the equilibrium vapor pressure must perforce be greater than $P_\infty(T)$. This means that even for supersaturations greater than unity the stable state of the finite system may be a pure gas rather than a liquid drop in equilibrium with its vapor.

What happens when gas imperfection is included? For simplicity we include only the second virial coefficient

$$B_2(T) = 2\pi \int_0^{r_0} r^2 (e^{-\beta\Phi(r)} - 1) dr \tag{14}$$

which is computed using the same potential used in our simulations (see Sec. III). Equation (15) can then be

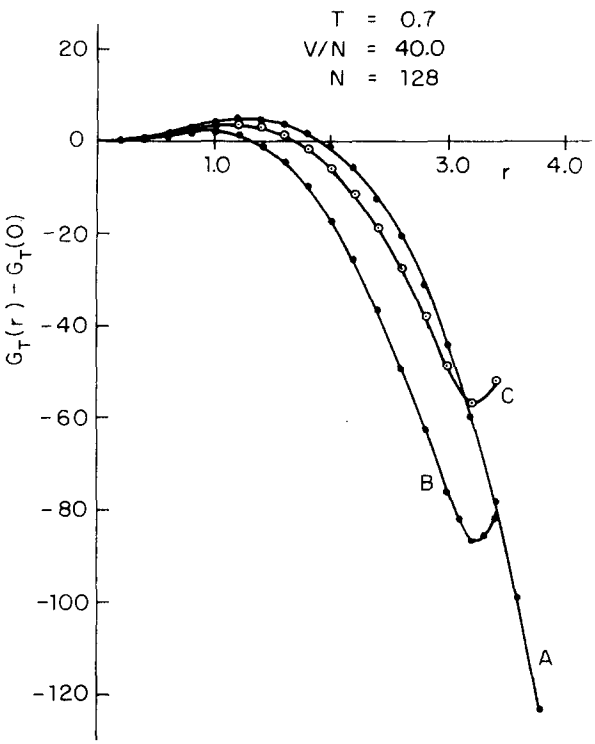

FIG. 2. Plot of excess free energy $[\Delta G_F(r)]$ for a 128 particle system $T=0.7$ at $V/N=40.0$. Curve A is given by classical nucleation theory with pressure held constant. Curve B is given by theory in Sec. II without virial correction. Curve C includes virial correction.

used to calculate $\Delta G_F(r)$. The equation again has a maximum and a minimum. In Fig. 2 $\Delta G_F(r)$ is plotted as a function of r. Line (A) indicates the free energy of formation in an infinite system where P is held constant. Line (B) gives the result for a perfect gas and Line (C) indicates what happens when non ideality is considered up to the second virial coefficient. At the low temperatures considered here intermolecular attractions make $B_2(T)$ strongly negative. From Fig. 2 we see that attractions between the gas molecules helps to destabilize the cluster by shifting r^* and ΔG_F^* to higher values and increasing the free energy of formation of the stable cluster. To be self-consistent, attractions between the cluster and the gas atoms should be included. Similar calculations give the stable cluster size as a function of V/N.

Here we have been considering the formation of droplets in supersaturated gases. At the opposite extreme there is the metastability associated with the over expansion of a liquid. If a liquid is initially at a pressure $P>P_\infty(T)$, no vapor will exist. Reversible expansion of the liquid reduces the pressure to $P_\infty(T)$, at which point vapor should form. Actually the liquid can be expanded (overexpanded) to a metastable state with $P<P_\infty(T)$. In this state cavities form in the liquid, but before vaporization can occur gas bubbles must form. Again there is a barrier to the nucleation of these bubbles. At low enough temperatures, the pressure of an overexpanded liquid can be negative. In the computer simulations to be described this behavior is observed.

This simple model gives us an insight into what happens in a simulation. For given values of N, V, and T, it is possible to simulate a stable cluster in equilibrium with its vapor and study its thermodynamics. As long as the cluster is far away from the boundaries the thermodynamics of the cluster are unchanged whether hard walls or periodic boundary conditions are used. However, using periodic boundary conditions one has the added advantage of studying the uniform liquid phase and cavitation for small volumes (see Fig. 3). The major defect of the simple model is the use of the macroscopic properties of a liquid and the omission of relative interactions between the droplet and the vapor.

III. METHODOLOGY

Molecular dynamics (M.D.) and Monte Carlo (M.C.) simulations have been carried out on systems containing 128 and 256 particles interacting via a truncated Lennard-Jones (12, 6) potential

$$\begin{aligned}\Phi(r) &= V(r) - V(r_0) \qquad 0 \le r \le r_0 \\ &= 0 \qquad\qquad\qquad r > r_0 ,\end{aligned} \tag{15}$$

where

$$V(r) = 4\epsilon\left[\left(\frac{\sigma}{r}\right)^{12} - \left(\frac{\sigma}{r}\right)^{6}\right], \tag{16}$$

and the cutoff distance $r_0 = 2.5\sigma$. In addition σ, ϵ, and $\tau_0\,[=(m\sigma^2/48\epsilon)^{1/2}]$ are chosen as length, energy, and time units (for liquid argon $\sigma = 3.405$ Å, $\epsilon = 119.4$ °K, and $\tau_0 = 3.11\times10^{-13}$ sec).

In the M.D. studies the particles are placed in a fully periodic box of size $L\times L\times L$ [see Fig. 4(a)], with a Maxwellian distribution of velocities corresponding to a mean temperature of 0.7 (84 °K). This temperature is chosen because the density profile, surface tension, $P_\infty(T)$, etc., in the case of a flat interface are already known from M.D. simulations for the potential given in Eq. (11). The integration time step is chosen to be

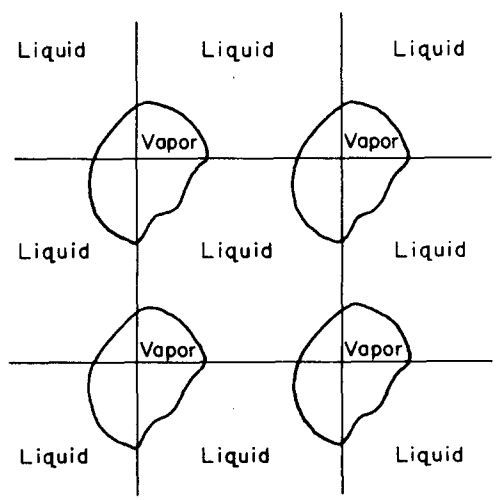

FIG. 3. Example of cavitation. The bubble shown can either be a vacuum or contain vapor. Using the periodic boundary conditions the cavitation is caused by the attraction of the image droplets.

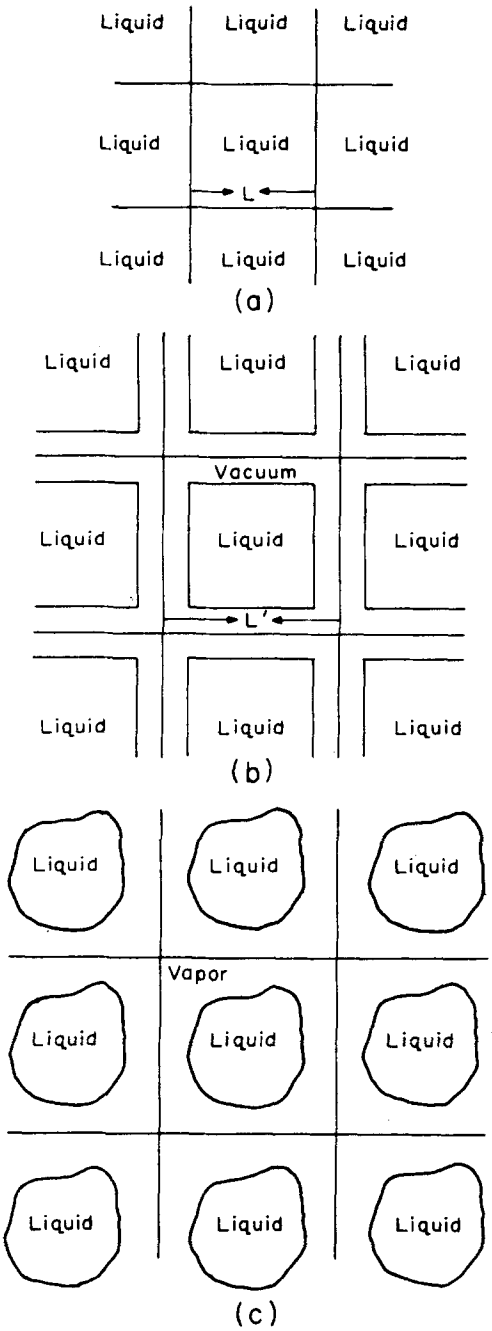

FIG. 4. (a) Periodic cells of size L containing liquid after equilibrium has been established. (b) Size L is changed to L' without changing the coordinates of the liquid particles, thus creating a vacuum. The evolution is continued until equilibrium is establlished. (c) Liquid droplet coexisting with vapor after equilibrium is established.

$0.032r_0$. Starting from a fcc lattice configuration, the system is allowed to age to an equilibrium configuration in the periodic box. Next the sides of the periodic cube are increased from L to L' [as shown in Fig. 4(b)] without changing the particle coordinates in any way. This generates an infinite array of cubic droplets. The average density $\bar{n}$ thus changes from N/L^3 to N/L'^3. Time evolution is then continued until equilibrium is re-established [see Fig. 4(c)]. During the initial phases of this time evolution particles evaporate from the cubical droplets. The temperature of the system decreases during the evolution due to evaporation and the kinetic energy is adjusted periodically (every ~2000 time steps) to maintain a constant temperature of 0.7 at equilibrium. After equilibrium is established (showing constant temperature and pressure within statistical error over 4000 time steps) the evolution is continued further to obtain the density profile $n(r)$ and the energy profile $e(r)$. These profiles are defined as follows: $n(r)4\pi r^2\Delta r$ gives the number of particles within a shell of width Δr at a distance of r from the center of gravity. $n(r)$ is obtained by counting the number of particles in a given shell and dividing by the volume of the shell. The shell thickness is taken to be $\Delta r = 0.4$. $e(r)$ is the average potential energy of a particle within this shell due to all other particles that are within the cut off distance r_0. These profiles show the existence of a stable cluster of liquid at the center of gravity surrounded by monomers, dimers, etc., constituting the vapor.

The procedure outlined above is also followed using the Monte Carlo method to make sure that what we are observing is indeed an equilibrium state. The usual Metropolis *et al.*[12] scheme is used with a step size of 0.2 for the random walk. Within statistical errors the results obtained by both methods are identical. However, for large volumes corresponding to small average density the Monte Carlo method is more efficient since molecular dynamics takes more computer time to stabilize the temperature fluctuations due to evaporation and condensation. On the other hand, molecular dynamics gives the time evolution of the system which is essential in understanding the kinetic processes. Thus both methods are used here to complement each other.

It is important to devise a method for counting clusters. Originally we identified a cluster as an assembly of particles such that each particle in the assembly has a potential energy lower than a certain value, say, $e_0(<0)$. Since vapor particles have potential energies close to zero, judicious choices of e_0 could be made such that the resulting cluster distribution are invariant to a fairly wide range of choices for e_0. Although the approach is useful, we finally adopted Stillinger's definitions[13] of a cluster: if any particle lies within a cut off distance r_c of another particle, the two particles are said to belong to the same cluster. This is described in Fig. 5. It is also possible to give a graphical description of this definition. To this end consider each pair of atoms in a particular configuration of the N particle system. If two atoms of a pair lie within r_c of each other a line is drawn between them. A cluster is then defined as a set of atoms that is at least singly connected by such lines. Thus within a cluster there will be at least one connected path between any two particles. The N-particle configuration can then be naturally subdivided into distinct clusters—clusters that are not connected by any lines—and the numbers of monomers, dimers, etc., can be counted. With this definition it is possible to study not only the dynamics of "physical clusters" but also the kinetics of recombination, dissociation, etc. In Fig. 5, we show a two-dimensional schematic of this cluster definition. Of course, this choice becomes

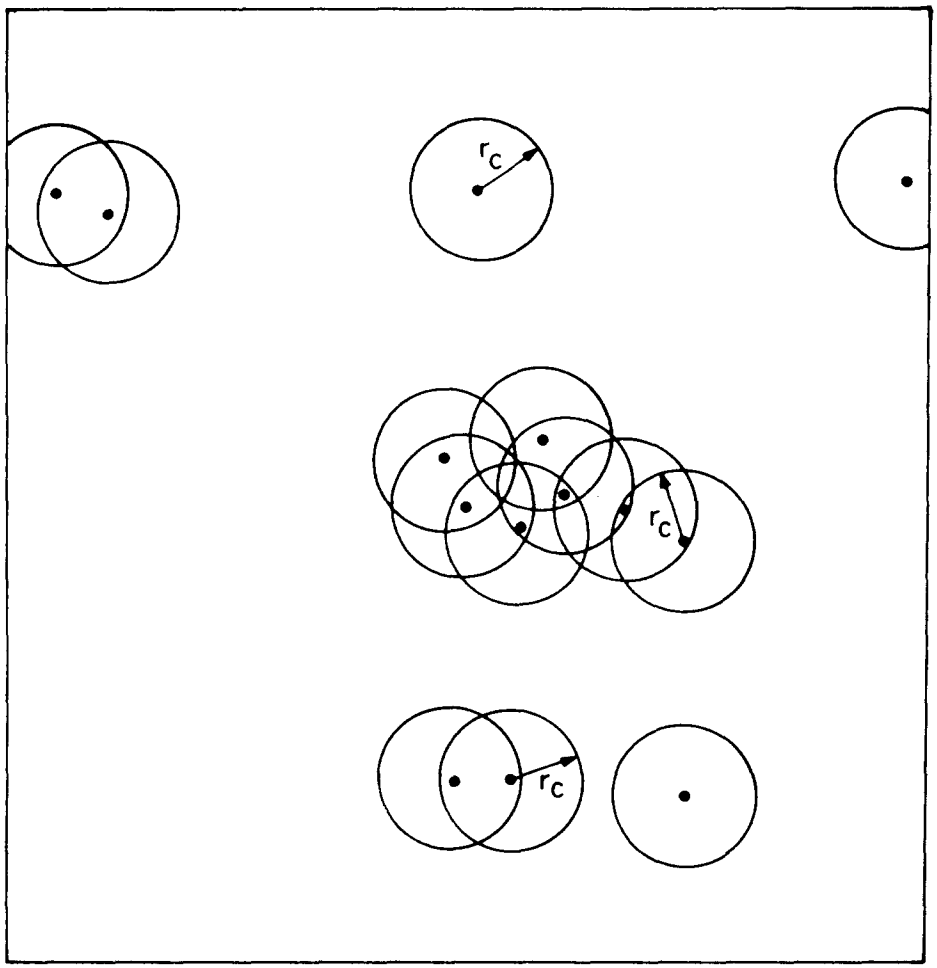

FIG. 5. Schematic illustration of the cluster definition (two dimensional!).

useless if the observed cluster distributions averaged over a number of configurations is very sensitive to r_c. Fortunately, it is experimentally observed that the cluster size and the distribution do not depend very sensitively on the choice of r_c. In fact, little change is observed when r_c is varied from 1.7σ to 2.5σ. We have chosen $r_c = 2.0\sigma$ with $r_0 = 2.5\sigma$. With this choice of cluster definition each configuration is analyzed to obtain a cluster distribution.

An average cluster distribution is obtained by an ensemble average over many configurations. If $N(l)$ is the number of clusters of size l, then for a fixed number of atoms in the system

$$\sum_l lN(l) = N \,. \tag{17}$$

The probability of finding a cluster of size l is obviously

$$P(l) = \frac{N(l)}{\sum_l N(l)} \,. \tag{18}$$

To obtain meaningful cluster distributions large sampling times are required. The binding energies of various l-mers are studied by computing the potential energy of each particle in an l-mer due to all other particles within the cut off distance r_0 (not r_c). The cohesive energy $e(l)$ of the l-mer is defined as the sum of these potential energies. The virial pressure of the system is defined as

$$P = \frac{N}{V}kT - \frac{1}{6V}\left\langle \sum_{i\neq j} r_{ij}\frac{d\phi(|r_{ij}|)}{dr_{ij}} \right\rangle \,. \tag{19}$$

This definition includes the contributions from both the liquid and vapor phases. However, in the situations where a stable cluster is in equilibrium with vapor the contribution of the cluster to the virial pressure comes from the center of gravity motion of the cluster as a whole which is quite small. Hence to a good approximation virial pressure can be taken as a measure of the vapor pressure P_G.

Physical cluster theory gives an alternative expression for the total pressure

$$P = \frac{kT}{V}\sum_l N(l) \tag{20}$$

in terms of $N(l)$, the number of clusters of size l. This expression also contains a contribution from the center of mass motion of the droplet, so that $P_G = P - kT/V$. Yet another measure of the vapor pressure can be obtained by substituting Eq. (5) for the vapor density into the virial expansion Eq. (2). If terms beyond the second virial coefficient are dropped,

$$P_G = n_G kT[1 + B_2(T)n_G] \,, \tag{21}$$

where $B_2(T)$ is given by Eq. (14).

All three definitions of the pressure give the same

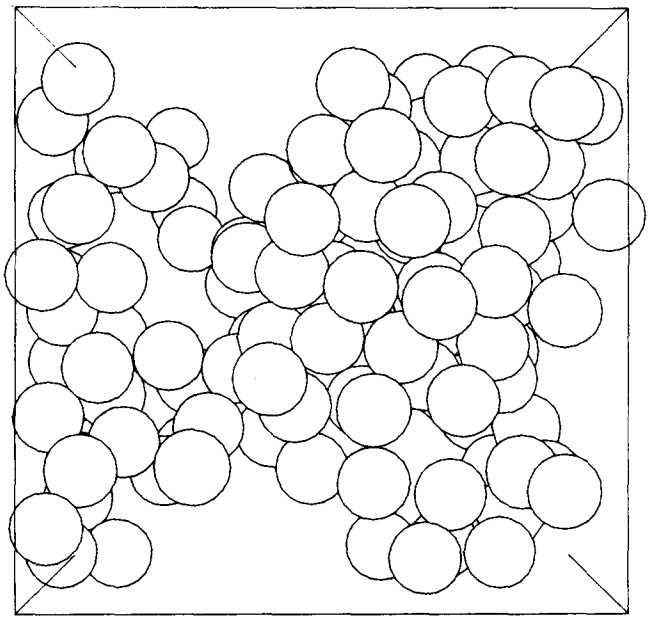

TAPE T714 IM 128 CONF 0 Z LIMITS -4.31 4.31

FIG. 6. Typical configuration after equilibrium has been established showing the stable cluster and vapor. $V/N=5$, $N=128$, $T=0.7$.

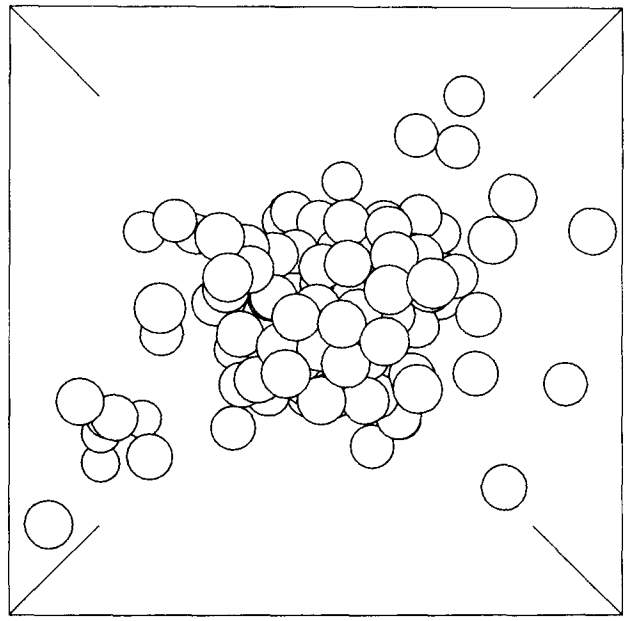

TAPE T714 IM 128 CONF 0 Z LIMITS -6.84 6.84

FIG. 8. Typical configuration after equilibrium has been established showing stable cluster and vapor. $V/N=20$, $N=128$, $T=0.7$.

value to within the statistical error of our simulations in the M.D. studies.

To insure that the apparent equilibrium state observed for a particular value of N, V, and T does not depend on the initial configuration we have also carried out a simulation starting from a low density uniform gas using both M.C. and M.D. After equilibration we observe essentially the same sized droplet and the same thermodynamic properties, $n(r)$, $e(r)$, and $P(l)$, indicating that we are observing a reproducible equilibrium state. To our knowledge this represents the first homogeneous nucleation in the gas phase generated on a computer. For higher values of V/N the barrier to nucleation may be sufficiently high that homogeneous nucleation would not be observed (see end of Sec. II). Then there would be hysteresis effects: that is, the final state starting from a saturated gas will be different from the final state starting from a critical liquid droplet.

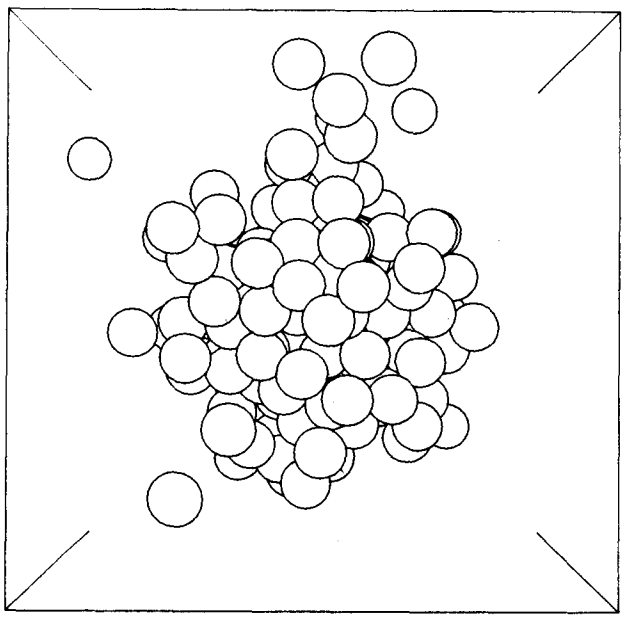

TAPE T714 IM 128 CONF 0 Z LIMITS -6.21 6.21

FIG. 7. Typical configuration after equilibrium has been established showing stable cluster and vapor $V/N=10$, $N=128$, $T=0.7$.

We must point out that care must be exercised in preparing the equilibrium stable cluster configurations in employing molecular dynamics. In molecular dynamics the total energy E is constant and this gives rise to different metastable cluster distributions with different potential energy configurations for the same temperature. However, the equilibrium state corresponds to the lowest energy E for a particular temperature and reaching this state can be a long process when one starts out with uniform gas phase. Adjusting the temperature to be constant over a reasonable period of time can also be very time consuming. Monte Carlo has the advantage that temperature remains fixed and the lowest energy state is obtained naturally. It has the disadvantage that time dependent properties cannot be studied.

The experiment is repeated for various values of the size of the periodic box L. For some values of L both M.D. and M.C. simulations are compared to establish that the same equilibrium state is observed, despite the existence of temperature fluctuations.

IV. RESULTS

The results of our simulation completely support the feasibility of studying stable "physical clusters" using both Monte Carlo and molecular dynamics. Figures 6–10 represent typical configurations of a 128 particle

system corresponding to various values of the average density N/V. When periodic boundary conditions are used we simulate a uniform one phase system for small values of V/N. As V/N increases the system commences to evolve into the two phase region. The binding attraction of the liquid phase in the primary cell is cancelled by the attraction of the image droplets thus giving rise to "cavitation." If there is enough free volume in the cavity (depending on V/N) vapor is trapped in the cavity and vapor bubbles are formed. For large values of V/N the liquid phase in the primary cell ceases to interact with its images due to the finite range of the cutoff potential and we have a well-defined liquid droplet in equilibrium with its own vapor. In this regime the main competing events in the formation of the droplet are the evaporation and condensation. Figures 11(a) and 11(b) represent a typical number distribution of clusters of size l for a given value of V/N in a 128 particle system averaged over seven independent simulations each with 512 128 Monte Carlo moves after equilibrium has been established.

In Figs. 12(a) and 12(b) the corresponding values of $n(r)$ and $e(r)$ are plotted as a function of r, the distance from the center of gravity of the stable cluster. Within statistical errors the liquid phase has the same density as that of the bulk liquid in equilibrium with vapor. For a comparison the density and energy profile found by M.D. for a infinite planar interface is also indicated on Figs. 12(a) and 12(b). It is important to note that the droplet interface looks much like the planar interface. Thus we would not be surprised if further analysis indicated that the capilarity waves observed in the planar case also characterize the surface of a spherical droplet. Because the vapor pressure of a spherical droplet must be larger than that of a plane sheet, the vapor density of the droplet must also be higher than the sheets. This is also clearly indicated in Fig. 12(a).

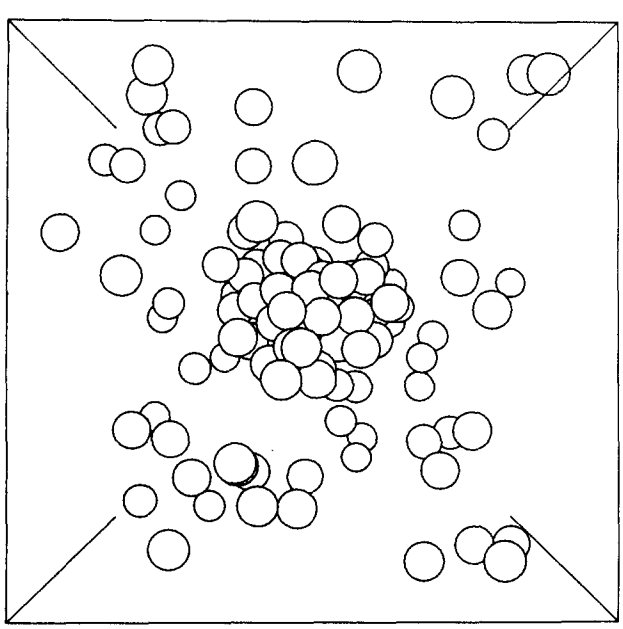

FIG. 9. Typical configuration after equilibrium has been established showing stable cluster and vapor. $V/N=40.0$, $N=128$, $T=0.7$.

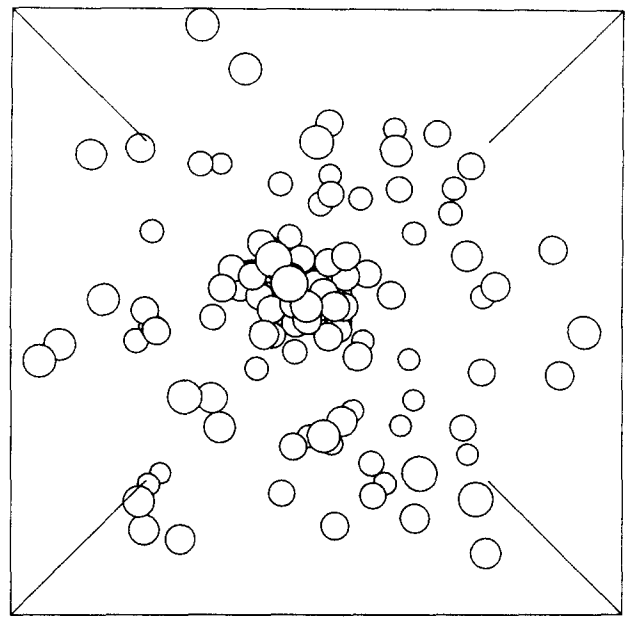

FIG. 10. Typical configuration after equilibrium has been established showing stable cluster and vapor. $V/N=90.0$, $N=128$, $T=0.7$.

The vapor phase consists of monomers, dimers, trimers, etc. [Fig. 11(a)]. The peaks in the two distributions correspond to the energy minima in Fig. 1 indicating the vapor phase and the stable cluster. It is important to note that in none of these seven independent runs did we ever observe a cluster of size greater than 10 and less than 89 after equilibrium has been established. This shows that it is energetically unfavorable to form a cluster in the steeply descending portion of the curve in Fig. 1.

In Figs. 13(a), 13(b), and 13(c) the virial pressure of the total system is plotted as a function of V/N for $N=128$ and $N=256$. This pressure corresponds to the interaction potential given in Eq. (15). In a homogeneous system it is straightforward to apply the usual tail corrections to thermodynamic properties like pressure, energy, etc., obtained from the truncated potential to compare with those values corresponding to a liquid with an infinite range potential. In a nonuniform system where the distribution functions change significantly in the interface region such *a posteriori* corrections are complicated, if possible at all, and consequently are not attempted here. The dots denote M.D. results and crosses denote M.C. results. For small values of V/N, the pressure is greater than $P_\infty(T)$ and the system corresponds to a one phase liquid region. When $P<P_\infty(T)$ cavitation starts to take the system into a two phase region. However, until the cavities formed reach a critical size to support vapor bubbles the pressure decreases as a function of V/N. When vapor bubbles form, the pressure increases with volume. For large values

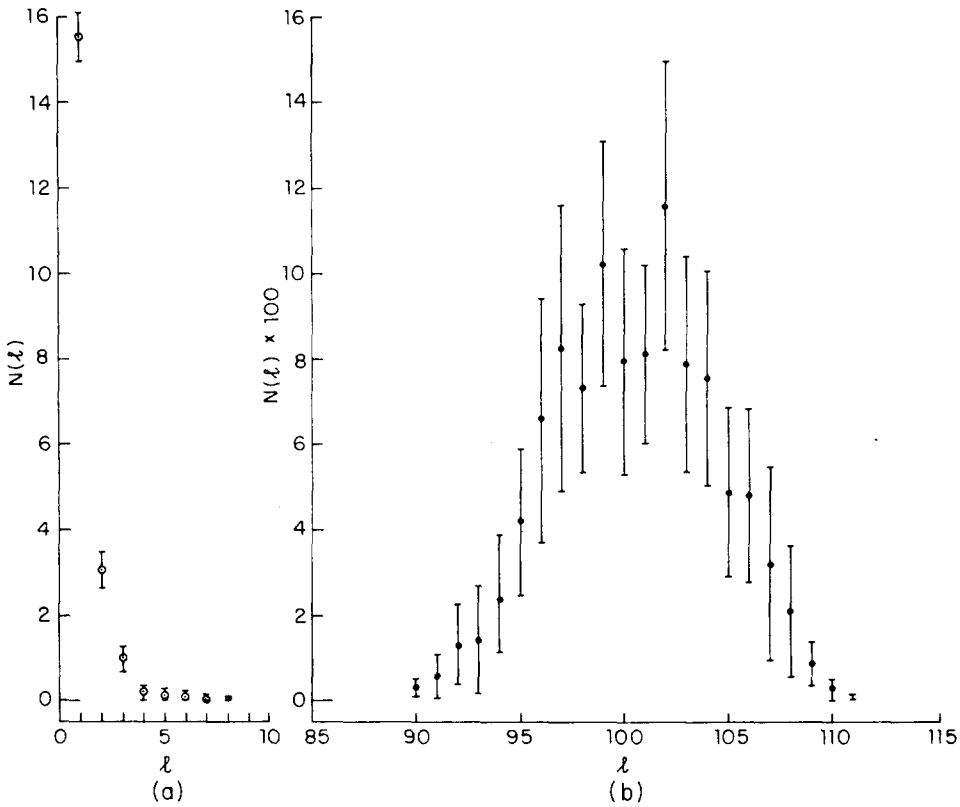

FIG. 11. (a) Distribution of monomers, dimers, etc., constituting the vapor phase averaged over seven runs each with 512 128 Monte Carlo moves after equilibrium has been established in a 128 particle system with $V/N=20.0$ $T=0.7$. (b) Distribution of the stable cluster for the same system as in Fig. 10 (a).

of V/N the droplet ceases to interact with its images and a stable cluster in equilibrium with its own vapor is created. The pressure is larger than $P_\infty(T)$ and decreases with V/N. As the volume increases the free energy corresponding to the stable cluster reaches a value larger than that of the uniform gas phase. If the minimum is still pronounced a metastable state is reached and the simulation of this state depends on the choice of the initial configuration. Lifetimes and kinetics of such states can be studied using molecular dynamics to understand the approach to equilibrium. Eventually for a very large value of V/N supersaturated vapor phase is established with only a distribution of small clusters. The near cancellation of the kinetic and potential contribution to the virial pressure makes the error in the determination of pressure quite large.

We define $\langle l\rangle = \sum_{l>10} N(l)l/\sum_{l>10} N(l)$, which yields a measure of the "stable cluster" size corresponding to this average density. Figures 14(a) and 14(b) show the variation of $\langle l\rangle/N$ with V/N. The decrease in the stable cluster size with increasing V/N is qualitatively consistent with the simple picture presented in Sec. II. The stable cluster size as a function of V/N using the second virial correction is shown in Fig. 14(a) with a solid line. Theory gives a value of $\langle l\rangle/N$ that is too large. Inclusion of higher virial coefficients should destabilize the droplet and lead to lower values of $\langle l\rangle/N$. However, because the values of $B_3(T)$ were not calculated we cannot give any quantitative statement of this. Another improvement would be to use the surface tension for a droplet of radius r in place of the surface tension of a planar interface. We note in passing that an attempt to improve the simple model using Tolman's correction

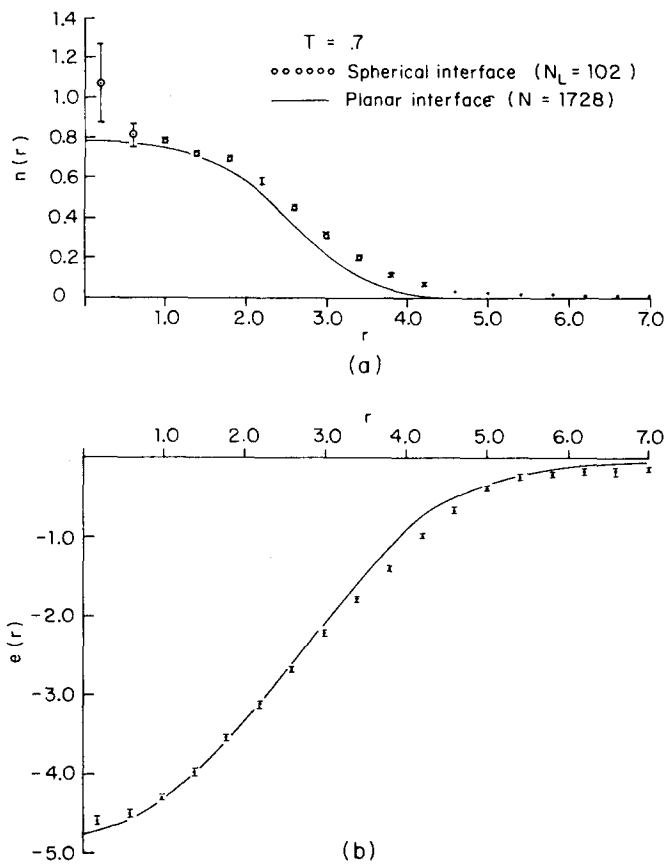

FIG. 12. (a) Density profile $n(r)$ as a function of r for the same system as in 10 (a). Solid line is for planar interface, circles are for droplet. (b) Energy/particle as a function of r for the same system as in 10 (a). Solid line is for planar interface, circles are for droplet.

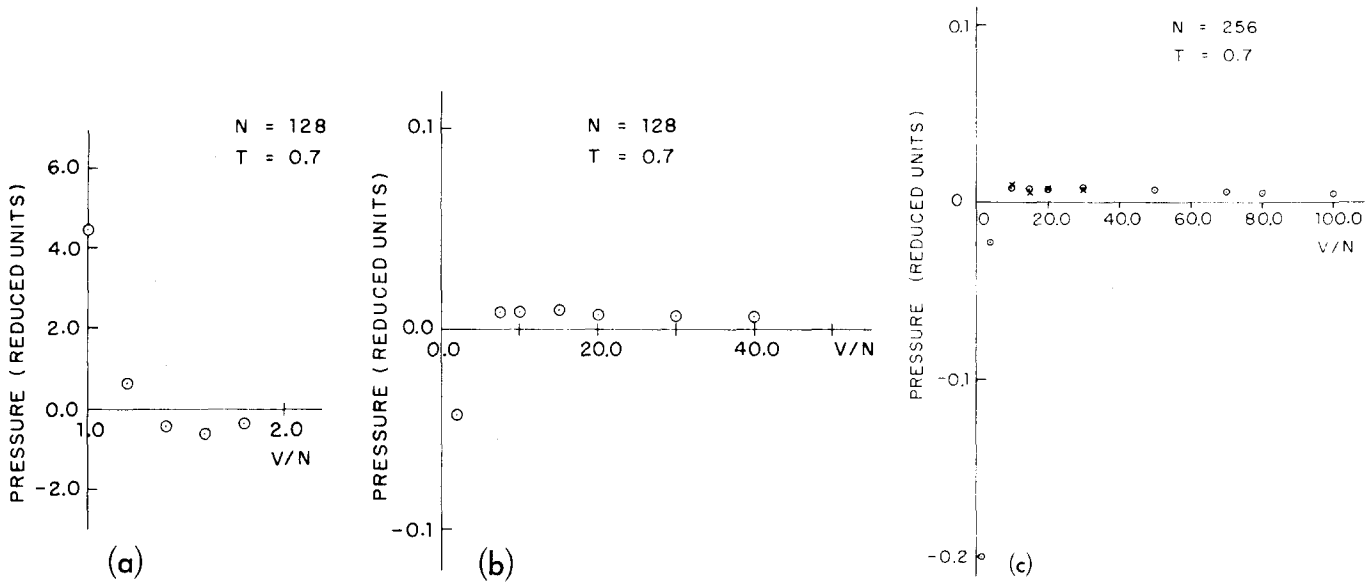

FIG. 13. (a) Virial pressure as a function of V/N for a 128 particle system $T=0.7$. Monte Carlo results (small values of V/N). (b) Virial pressure as a function of V/N for a 128 particle system $T=0.7$. Monte Carlo results (large values of V/N). (c) Virial pressure as a function of V/N for a 256 particle system $T=0.7$. Crosses denote Monte Carlo results and circles denote Molecular dynamics results.

for surface tension was unseccessful. Probably any theory that tries to explain quantitatively properties of small finite systems on the basis of macroscopic thermodynamics is destined to fail.

We have also measured the structure factor $S(k)$ for the whole system,

$$S(k)=\frac{1}{N}\left\langle \sum_{i,j} e^{i\mathbf{k}(\mathbf{r}_i-\mathbf{r}_j)} \right\rangle , \tag{17'}$$

for the smallest wave vector allowed by the periodic boundary conditions. This gives a measure of the stable cluster size and is in quite good agreement with that obtained from our cluster definition. In the case of large clusters one can study this quantity as a function of the distance from center of gravity and study the correlations that exist in the surface. It will be useful to understand the effect of curvature on the long range correlations that exist in the case of a flat interface.

V. CONCLUSION

This is the first of a series of papers that will be devoted to understanding the thermodynamics, kinetics, and structure of the liquid–vapor interface in droplets of liquid, using computer simulation. These studies are important not only for their own merit but also in understanding nucleation phenomena. In the present paper we have demonstrated the feasibility of preparing small stable droplets in equilibrium with vapor, and have studied their thermodynamics and structure. We have shown that using the usual periodic boundary conditions we can indeed study not only the uniform phase but also stable clusters of any size. Employing this scheme we avoid the objections raised against other methods like the one employing a constraining volume. Our definition of the cluster ensures that all atoms are actually bound to the cluster by the binding forces and

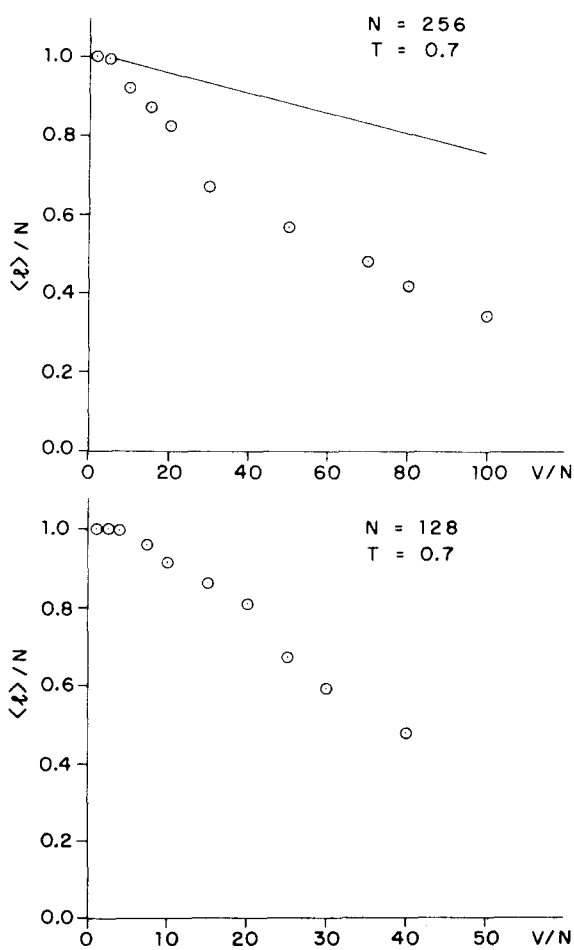

FIG. 14. (a) Average stable cluster size $\langle l\rangle/N$ as a function of V/N for a 256 particle system $T=0.7$. The line denotes the theory discussed in Sec. II with second virial correction. (b) Average stable cluster size $\langle l\rangle/N$ as a function of V/N for a 128 particle system. $T=0.7$.

that the motion of the cluster occurs as a whole. Employing molecular dynamics we can also study kinetic processes like evaporation, condensation dissociation, recombination, diffusion, etc., of these clusters which are of great importance in understanding the nucleation phenomena.

This study has been restricted to the study of small droplets. However, we are at present extending these methods to the study of big droplets. When the droplet size is large enough so that there is an appreciable amount of liquid phase in the interior, surface tension remains a valid concept and it will be interesting to study the surface tension obtained from the one particle and the two particle distribution functions $P(|r|)$ and $P(r_1 r_2)$ which can be measured readily from simulation. These studies will give a better understanding of how surface tension depends on radius. These corrections also might play an important role in understanding the variation of cluster size with V/N.

The feasibility of simulating inhomogeneous systems consisting of droplets in equilibrium with vapor sets the stage for several interesting studies of microclusters. The theoretical model presented here is clearly overly simplistic; nevertheless, it suggests that in finite systems there is still a barrier to nucleation, and that in addition there exists a stable equilibrium state consisting of a microcluster in equilibrium with vapor. The theoretical model is entirely thermodynamic and therefore fails to account for the large fluctuations present in small systems. Obviously the theory can be improved by following the approach outlined by Hill.[14]

It is important to recognize that when there is an interface, the properties of the system depend strongly on the attractive potential. Comparing the truncated and full L-J (12–6) potential it is clear that the cohesive energy e as well as the bulk fluid density n_L are larger for the full potential than for the truncated potential whereas the equilibrium vapor pressure is smaller for the full potential than for the truncated potential. It is also possible to infer that the density gradient in the interfacial region is greater for the full potential than for the truncated potential. Recently, Miyazaki *et al.*[15] has determined that the surface tension σ for the full potential is $\sigma = 18.2$ dyn/cm (argon units). This is considerably larger than $\sigma = 12$ dyn/cm for the truncated potential. Liquid argon has $\sigma = 13$ dyn/cm. Thus the agreement between the truncated potential and the real liquid must be regarded as fortuitous. This clearly indicates that simulations of systems with interfaces provide a much more sensitive test of the intermolecular potential than do simulations of uniform systems. It shows moreover that the Lennard-Jones (12–6) potential, despite its success in accounting for the bulk properties of uniform liquid argon, is a poor potential for studies of phase equilibria. Given the foregoing, we must regard this paper as a study of a well-defined model fluid rather than of any real fluid. Nevertheless, we expect that our discussion is still applicable in a qualitative sense to real fluids. When discussing surface properties it is important to be aware of the fact that the interfacial profile is strongly dependent on the dimensions of the surface. In a recent paper Weeks[16] has shown that the thickness of the interfacial region increases without bound as the surface area approaches infinity. Recently Rowlinson *et al.*[17] have performed molecular dynamics studies on systems with different surface areas. Their results are consistent with the view advanced by Weeks. Given this size dependence it is important to ask why the surface profile of a droplet is so similar to that of a planar sheet—a similarity clearly indicated in Fig. 12(a). Although it may not be obvious, each edge of the planar surface is $\sim 12\sigma$, whereas the circumference of the droplet is $\sim 12\sigma$. Thus the longest wavelength capilarity waves that can be supported by the planar surface and by the droplet surface have approximately the same wavelength. For this reason we expect the interfacial profiles of these two different systems to be quite similar despite the fact that the planar sheet has 1728 particles whereas the droplet has 128 particles.

Several points worth noting in conclusion are as follows:

(a) The density profile in microclusters looks very much as it does in the interfacial region of an infinite sheet. It thus seems reasonable that the droplet interface can also be described by capilary waves.

(b) At high supersaturation the barrier to nucleation is sufficiently low that we are able to observe homogeneous droplet nucleation in Monte Carlo and molecular dynamics simulations.

(c) Nucleation takes place, and droplets grow under essentially adiabatic conditions; that is, collisions of the microcluster with vapor are sufficiently infrequent that due to latent heat effects the temperature of the droplet increases. In nucleation theory the process is assumed to be isothermal—an assumption that should be modified. This observation should apply to nucleation in other systems only when the thermal contact between the two phases is sufficiently weak that the latent heat is not removed rapidly enough by thermal conduction. There is evidence that this is the case in freezing in argon.

(d) Cavitation processes in the overexpansion of a liquid, at low enough temperatures gives rise to negative pressures. We have been able to observe the transition between cavitation and droplet formation. Theory has yet to be developed to explain at what overexpanded volume this will occur.

(e) Vapor imperfection increases both the barrier height and the critical cluster size and destabilizes equilibrium droplet formation.

(f) The P–V diagram has a loop that reflects the barrier to cavitation or bubble formation and the barrier to droplet formation. What in an infinite system would be regarded as the unstable part of the loop is stabilized in a finite system by surface energy effects.

[1]J. K. Lee, T. A. Barker, and F. F. Abraham, J. Chem. Phys. 58, 3166 (1973); F. F. Abraham, J. Chem. Phys. 61, 1221 (1974).
[2]J. K. Lee, J. A. Barker, and G. M. Pound, J. Chem. Phys. 60, 4226 (1974).
[3]K. S. Liu, J. Chem. Phys. 60, 1976 (1974).
[4]G. A. Chapela, G. Saville, and J. S. Rowlinson, Discuss. Faraday Soc. 59, 22 (1975).
[5]F. F. Abraham, D. E. Schreiber, and J. A. Barker, J. Chem. Phys. 62, 1958 (1975).
[6]M. Rao and D. Levesque, J. Chem. Phys. 65, 3233 (1976).
[7]M. H. Kalos, J. K. Percus, and M. Rao, J. Stat. Phys. 17, 111 (1977).
[8]F. F. Abraham, *Homogeneous Nucleation Theory* (Academic, New York, 1974).
[9]K. Binder, J. Chem. Phys. 63, 2265 (1975).
[10]F. F. Abraham and J. A. Barker, J. Chem. Phys. 63, 2266 (1975).
[11]J. J. Burton, *Statistical Mechanics Part A: Equilibrium Techniques*, edited by B. J. Berne (Plenum, New York, 1977), and references therein.
[12]N. Metropolis, A. W. Metropolis, M. N. Rosenbluth, A. H. Teller, and E. Teller, J. Chem. Phys. 21, 1087 (1953).
[13]F. H. Stillinger, Jr., J. Chem. Phys. 38, 1486 (1963).
[14]T. L. Hill, *Thermodynamics of Small Systems* (Benjamin, New York, 1963).
[15]J. Miyazaki, J. A. Barker, and G. M. Pound, J. Chem. Phys. 64, 3364 (1976).
[16]J. D. Weeks, J. Chem. Phys. 7, 3106 (1977); also see Ref. 7.
[17]G. A. Chapela, G. Saville, S. M. Thompson, and J. S. Rowlinson, J. Chem. Soc. Faraday Trans. 2 73, 1133 (1977).